THE UNIVERSITY OF ALABAMA IN HUNTSVILLE

Semi-annual progress report
November 1, 1990 - April 30, 1991

NAGW-2128

"A New Approach to Plasmasphere Refilling: Anomalous Plasma Effects"

Prepared by

N. Singh, Ph.D.
Principal Investigator
Department of Electrical & Computer Engineering
College of Engineering
The University of Alabama in Huntsville
Huntsville, AL 35899

WORK PERFORMED

During the last 10 months of the grant we have investigated both laminar and anomalous plasma processes occurring during the refilling of the outer plasmasphere after magnetic storms. Our theoretical investigations have been based on two types of models: (1) two–stream hydrodynamic model in which plasma flows from the conjugate ionospheres are treated as separate fluids [Singh, 1988; Rasmussen and Schunk, 1988; Singh, 1990a] and the ion temperature anisotropies are treated self-consistently [Singh and Torr, 1990; Singh, 1990b; 1991], (2) large–scale particle–in–cell code [Wilson et al., 1990; Horwitz et al., 1990]. We briefly describe here our findings.

Temperature Anisotropy (TAN) Model:

In view of the observations that temperature anisotropies are endemic to the magnetic field–aligned flows of the thermal plasma in the outer plasmasphere [Young, 1983], we have extended the previous two–stream hydrodynamic models [Singh, 1988; Rasmussen and Schunk, 1988, Singh, 1990a] to include the ion temperature anisotropy by solving separate equations for the temperatures associated with the motions of ions parallel and perpendicular to the magnetic field. The relevant equations which we solve for each plasma stream along a closed field line (Fig. 1) are

$$\frac{\partial N_i}{\partial t} + \frac{\partial}{\partial s}(N_i V_i) = -N_i V_i \frac{1}{A}\frac{\partial A}{\partial s} \tag{1}$$

$$\frac{\partial V_i}{\partial t} + \frac{\partial}{\partial s}\left(\frac{1}{2} V_i V_i\right) = \frac{q_i}{m_i} E - \frac{k_b}{m_i}\frac{\partial T_{\|i}}{\partial s}$$

$$- \frac{k_b}{m_i} T_{\|i} \frac{1}{N_i}\frac{\partial N_i}{\partial s} - g_{\|} - \frac{k_b}{m_i}(T_{\|i} - T_{\perp i})\frac{1}{A}\frac{\partial A}{\partial s} + \left[\frac{\partial V_i}{\partial t}\right]_c \tag{2}$$

$$\frac{\partial T_{\|i}}{\partial t} + \frac{\partial}{\partial s}(V_a T_{\|i}) = - T_{\|i}\frac{\partial V_i}{\partial s} + \left[\frac{\delta T_{\|i}}{\delta t}\right]_c - \frac{1}{A}\frac{\partial}{\partial s}\left[A q_{\|i}\right] \tag{3}$$

$$\frac{\partial T_{\perp i}}{\partial t} + \frac{\partial}{\partial s}(V_a T_{\perp i}) = T_{\perp i}\frac{\partial V_i}{\partial s} - T_{\perp i} V_i \frac{1}{A} + \left[\frac{\delta T_{\perp i}}{\delta t}\right]_{Turb}\left[\frac{\delta T_{\perp i}}{\delta t}\right]_c - \frac{1}{A}\frac{\partial}{\partial s}\left[A q_{\perp i}\right] \tag{4}$$

where s is the distance along the field line from a ionospheric boundary (Figure 1), A is the cross–sectional area of the flux tube; $A \propto B^{-1}$, B is the magnetic field magnitude; q_i and m_i are the charge and mass of an ion. The subscript 'i' stands for the streams originating from the northern (i = n) or southern (i = s) ionospheres. These streams are treated as separate fluids [Singh, 1988]. V_i and N_i are the flow velocity and the density. $T_{\|i}$ and $T_{\perp i}$ are the parallel and perpendicular temperatures and $q_{\|i}$ and $q_{\perp i}$ are, respectively, the heat flows associated with $T_{\|i}$ and $T_{\perp i}$, along the magnetic field lines.

The interstream collision terms $(\delta F/\delta t)_c$ appearing in the equations for V_i, $T_{\|i}$ and $T_{\perp i}$ are similar to those given by Burger [1969], but the self–collisions which are effective

in relaxation of temperature anisotropy are given by [Ichimaru, 1973]

$$\left[\frac{\delta T_\perp}{\delta t}\right]_{ii} = -\frac{1}{2}\left[\frac{\delta T_\parallel}{\delta t}\right]_{ii} = -(T_{\perp i} - T_{\parallel i})\,\tau_i^{-1} \tag{5}$$

$$\tau_i^{-1} = \frac{8\pi^{1/2} N_i e^4}{15 m_i^{1/2} T_{eff}^{3/2}}\,\ell n\,\Lambda \tag{6}$$

$$\tau_{eff}^{-3/2} = \frac{15}{4}\int_{-1}^{1} d\mu\, \frac{\mu^2(1-\mu^2)}{[(1-\mu^2)T_{\perp i} + \mu^2 T_{\perp i}]^{3/2}} \tag{7}$$

When needed, the heating term $(\delta T_\perp/\delta t)_{Turb}$ appearing in (4) is chosen to represent ion heating by broadband waves in the limit of long wavelength waves;

$$\left[\frac{\delta T_\perp}{\delta t}\right]_{Turb} \simeq \frac{1}{4}\frac{q^2}{m_i}\,\psi \tag{8}$$

where ψ is the wave power spectral density in units of $V^2 m^{-2}$ Hz^{-1} [Singh and Schunk, 1984; Chang et al., 1986].

In a collision–dominated plasma, it is possible to describe the heat flows $q_{\perp i}$ and $q_{\parallel i}$ in terms of the thermal conductivities [Holzer et al., 1972]. In a collisionless situation, like that in the initial stage of the refilling it is not obvious how to calculate heat flows. It is possible that one can solve additional time–dependent heat flow equations [Mitchell and Palmadesso, 1983; Ganguli and Palmadesso, 1987], but it turns out to be quite tricky to solve such equations numerically [Palmadesso et al., 1988].

In a collisionless situation the maximum heat flow is $q_{ti} = (nk_b T_{ti})\,V_{th}$ where 't' stands for parallel ($t \equiv \parallel$) or perpendicular ($t \equiv \perp$) directions. Note that the quantity in the parentheses in the expression for q_{ti} is the thermal energy density $nk_b T_{\parallel i}$ or $nk_b T_{\perp i}$ and V_{th} is the parallel thermal velocity given by $(k_b T_{\parallel i}/m_i)^{1/2}$. It is known that in a collisionless plasma the heat flows are likely to be severely limited by plasma instabilities [Manheimer, 1977]. In the solar wind literature such situations have been handled by assuming [Metzler et al., 1979]

$$q_{ti} \simeq \epsilon\,\eta\, n_i k_b T_{ti}\, V_{th} \tag{9}$$

where ϵ is ± 1 depending on the sign of the gradient in temperatures ($T_{\perp i}$ or $T_{\parallel i}$) and η is a heat flow reduction factor due to the plasma turbulence. The transition from the collision–dominated to the collisionless situation is handled by calculating an effective heat flow q_{eff} by

$$\frac{1}{q_{eff}} = \frac{1}{q_c} + \frac{1}{q_{t\alpha}} \tag{10}$$

where q_c is the heat flow associated with $T_\parallel$ or $T_\perp$ determined by the collision frequencies. In a collisionless plasma $q_c \to \infty$ and (10) gives $q_{eff} \simeq q_{t\alpha}$. On the other hand, in a collision dominated plasma when $q_c << q_{t\alpha}$, $q_{eff} = q_c$.

We note that the heat flow reduction factor is determined by the plasma turbulence. In large scale models, it is difficult to determine this factor quantitatively. Thus, it is used as a free parameter so that the predictions from the hydrodynamic model agree with observations or with more rigorous kinetic models. Thus, there is definite need to study the issue of heat flow in collisionless plasma using both kinetic and hydrodynamic models. This is a part of our proposed research described in section 3.1

The electric field E is calculated by assuming that the plasma remains quasi–neutral and the electrons obey the Boltzmann law; $E = -(k\ T_e/e)(1/n)(dn/dn)$ where $n = \Sigma_i\ n_i$. Electron temperature T_e is assumed to be constant equal to the ionospheric temperature T_o. The set of equations (1) to (4) are solved subject to the following initial and boundary conditions. At the initial time the flux tube is assumed to be highly depleted, a typical condition after geomagnetic storms. The depletion is represented by $n_i = n_o\ (\lambda,\ t = 0)\ (\sin \lambda/\sin\lambda_o)^\gamma$ with the minimum density limited to $10^{-4} n_o$, when n_o is the density at the ionospheric bases at $\lambda = \pm\lambda_o$ (Figure 1). Initial flow velocity $V_i\ (\lambda,\ t = 0) = 0$ and temperatures $T_\perp(\lambda,\ t = 0) = T_\perp(\lambda,\ t = 0) = T_o = 0.31$ eV. The sensitivity of the results to the initial conditions was examined and it was found that for a severely depleted flux tubes ($n_{eq} \simeq 1\ cm^{-3}$), the details of the initial conditions do not significantly affect the flow and the refilling scenarios [Singh, 1991]. Boundary conditions for the fluid from the northern hemisphere are: $n_n(\lambda = \lambda_o,\ t) = n_o$, $V_n(\lambda = \lambda_o,\ t) = 0$, $T_n(\lambda_o,\ t) = T_{\perp n}(\lambda_o,\ t) = T_o$; at the boundary $\lambda = -\lambda_o$ floating boundary conditions are applied. A set of similar boundary conditions are used for the fluid originating from the southern hemisphere but with the roles of $\pm\lambda_o$ interchanged.

The anisotropy force $\alpha(T_\perp - T_\parallel)$ in the momentum equation plays important roles in the refilling process. Usually the origin of this force is not clearly understood, therefore, we briefly describe it here.

2.1.1 The Physics Behind the Anisotropy Force:

The momentum equation contains a force term which is proportional to $(T_\parallel - T_\perp)\ \partial A/\partial s$. We call this force the Anisotropy force. Since this force is found to have a considerable affect on the refilling, we briefly describe here the physical origin of the force. The mirror force per unit volume is $F_m = -nkT_\perp \frac{1}{B}\frac{\partial B}{\partial s} = nkT_\perp \frac{1}{A}\frac{\partial A}{\partial s}$, where the cross–sectional area of the flux tube A which is proportional to B^{-1}. The other force which is relevant here is the pressure force, which is essentially the net momentum transfer across an area. This force is operative in both collisional and collisionless plasmas. The pressure force on an element of plasma in a diverging flux tube is

$$-\frac{\partial}{\partial s}(nkT_\parallel A)\ \delta s \tag{11}$$

where A is the area of the cross section of the tube and δs is the elemental length along the tube. The above force can be decomposed into two parts:

$$-A\ \delta s \frac{\partial}{\partial s}(nkT_\parallel) - nkT_\parallel\ (A\delta s)\frac{1}{A}\frac{\partial A}{\partial s} \tag{12}$$

Dividing the above force by $A\delta s$, the pressure force per unit volume becomes

$$F_p = -\frac{\partial}{\partial s}(nkT_{||}) - nkT_{||}\frac{1}{A}\frac{\partial A}{\partial s} \tag{13a}$$

Thus the sum of the mirror and pressure force per unit volume is

$$F = F_p + F_m = -\frac{\partial}{\partial s}(nkT_{||}) - nk(T_{||} - T_{\perp})\frac{1}{A}\frac{\partial A}{\partial s} \tag{13b}$$

The first term is the usual pressure term in the momentum equation for a uniform flux tube (B = constant). The second term is called the anisotropy force; in fact it is the combination of the mirror force and the partial pressure force arising due to the divergence in the flux tube. In an isotropic plasma the two terms in this so–called anisotropy force cancel out. But in an anisotropic plasma the force remains non–zero. When $T_{\perp} > T_{||}$ the force is upward as the mirror force. When $T_{||} > T_{\perp}$, this force is downward simply because the pressure on the top surface of a plasma element in a diverging flux tube acts on a larger area than that on its bottom surface.

Generation of Equatorially Trapped Ions and Their Effects on Refilling

Observations from DE-1 and SCATHA Satellites [Olsen, et. al., 1987] have shown the presence of equatorially trapped ions in the outer plasmaspheric flux tubes. Normally such ions are H^+ and they have perpendicular temperatures ($T_{\perp}$) in the range 5 - 100 eV and the temperature anisotropy $T_{\perp}/T_{||} \simeq 10$ - 50. Such ions occur in conjunction with a broadband electromagnetic noise over the frequency spectrum from ion-cyclotron frequency to the lower-hybrid frequency. Such waves are generated by the energetic ions in the equatorial region. It is worth pointing out that the production of trapped ions through their interactions with the waves generated by the energetic ions of plasma sheet and/or of ring current origins is an interesting example of hot-cold plasma interactions, where the cold plasma is supplied from the ionosphere through the field-aligned plasma flows. Recently Singh and Torr [1990] studied for the first time the effects of equatorial ion heating on interhemispheric plasma transport by solving a self-consistent set of plasma transport equations. Here we briefly summarize the results from our recent studies on the effects of ion heating on the refilling of the outer plasmasphere. The temperature anisotropies resulting from both the polar wind type of outflow from the conjugate ionospheres in an empty flux tube and the equatorial ion heating are found to have profound effects on the refilling. Since some of the results from this study are already published [Singh and Torr, 1990] or are in press [Singh, 1990b], we present here only the main conclusions of this study.

(1) The equatorial heating inhibits interhemispheric plasma exchange due to the large mirror force on the heated ions. The penetration of the flow originating from one hemisphere into the opposite one depends on the heating rate at the equator (Fig. 2).

(2) The stoppage of the flow just beyond the equator in the opposite hemisphere launches a shock wave which propagates down to the ionosphere of its origin (Fig. 2e to 2g). Through the passage of this shock, the supersonic flow subsides in the flux tube. The transit time of the shock is found to be only a few hours (~ 4-6 hours) for flux tubes with $4 \leq L \leq 6$.

(3) After the shock crosses the heating region, temperature anisotropy across it changes from $T_{\perp} > T_{||}$ near the equator to $T_{||} > T_{\perp}$ (Figs. 2g and 2h).

(4) In the region with $T_{||} > T_{\perp}$ the anisotropy force ($\alpha(T_{\perp} - T_{||})$) becomes downward and it prevents the flux tube from refilling (Fig. 2e).

(5) After the passage of the shock when the flow velocity becomes quite small, and Coulomb collisions begin to become effective, first near the ionospheric boundaries where the densities are relatively high, the temperature anisotropy $T_{||} > T_{\perp}$ begin to relax leading to $T_{||} \sim T_{\perp}$ (Fig. 2k and 2ℓ).

(6) When the anisotropy relaxes, a new plasma flux develops into the flux tube (Fig. 2j). This second stage of flow is generally subsonic.

(7) In the second stage the flux tube refills from bottom to top with a cold isotropic plasma (Figs. 2i, 2k and 2ℓ).

(8). As the flux tube refills a variety of temperature and density structures appear in the flux tube, some illustrative examples are shown in Fig. 3. In the late stage of the refilling the trapped ions with $T_{\perp} > T_{||}$ have a twin-peaked structure (Fig. 3c) and this type of temperature anisotropy is found to extend in latitude beyond the equatorial region [Olsen et al., 1987].

Refilling Time of a Flux Tube

In the previous section we saw a two–stage refilling consisting of supersonic and subsonic flows. A similar two–stage refilling occurs even when equatorial ion heating is not included. Here the temperature anisotropy $T_{||} > T_{\perp}$, which develops due to the supersonic nature of the flow in the depleted flux tube and which is further enhanced by the formation of a shock, plays a crucial role in determining the life time of the supersonic flow and, hence, in the refilling time of the flux tube. In several previous models temperature isotropy (TISO) is explicitly assumed [Singh et al., 1986; Rasmussen and Schunk, 1988; Guiter and Gombosi, 1990]. TISO models show a substantial refilling of the flux tube during the supersonic flows from the conjugate ionospheres. The refilling process from a TISO model is shown in Figure 4, which shows that by the time $t \simeq 12.3$ hours, the equatorial density $n_{eq} \simeq 400$ cm^{-3}. Rasmussen and Schunk [1988] reported a similar refilling in about 24 hours, but they did not include the energy equation in their solution. When the equation for the H^+ temperature is solved along with the continuity and momentum equations , the refilling is found to be even faster. This is primarily due to the enhancement of temperature behind the shock. The temperature enhancement leads to a faster shock velocity. Guiter and Gombosi [1990] noted a similar behavior of the shocks during refilling.

The refilling time predicted by the TISO model is too short in comparison to the observed time of several days [Park, 1970]. The TAN model described above in Section 2.1 predicts a much slower refilling process.

Figure 5 shows the evolution of the flow from the northern to the southern hemisphere. A similar flow develops in the opposite direction. The density profile (Fig. 5a) at $t = 0$ shows the state of the empty flux tube. By $t = 2.31$ hours, the flow has caused a substantial accumulation of plasma in the southern hemisphere. This accumulation occurs when the supersonic flow from the northern hemisphere encounters the relatively dense plasma in the southern hemisphere. The supersonic flow is slowed down by the Coulomb collisions and by polarization electric fields. The accumulated plasma evolves into a shock as seen at $t = 2.31$ hours from the density (Fig. 5a), velocity (Fig. 5b) and parallel temperature profiles (Fig. 5d). The shock first propagates upward to the equator and then downward to the ionosphere. Behind the shock $T_{||} > T_{\perp}$. Thus, the anisotropy force is downward, and the shock is accelerated downward and it reaches the ionospheric

boundary in a relatively short time of t = 4.61 hours. The transit time of the shock from the equator to the boundary is less than two hours. During the phase of the downward shock propagation, there is very little refilling. As a matter of fact, the flow behind the shock is downward as seen from the velocity profiles at t = 3.84 hours (Fig. 5b). This is in contrast to the refilling seen in the TISO model, which predicts a substantial refilling behind the shock (Fig. 4).

The TAN model shows a second stage of refilling if the Coulomb collisions become effective in isotropizing the temperature anisotropy. This begins near the ionospheric boundaries, where plasma density is relatively large. Figure 5e shows the state of the isotropization at t = 7.68 hours, when $T_\perp \simeq T_\parallel$ up to about $\lambda \gtrsim 30^\circ$ near the northern boundary. In response to this isotropization, flow develops from the ionosphere (Fig. 5g). In this stage the flow is generally subsonic. The evolution of the density profile of the flow from the northern ionosphere shows an expanding plasma front shown by the arrows in Fig. 5f. This plasma is found to be cold and isotropic with a temperature $T_\perp \simeq T_\parallel \simeq T_o$. The evolution of the total density in the flux tube is shown in Fig. 5h, which suggest a monotonic refilling. We find that at t = 153.69 hours ≈ 6 days, the equatorial density $n_{eq} \simeq 325$ cm^{-3}, which should be contrasted with $n_{eq} \simeq 400$ cm^{-3} in about 12 hours as predicted from the TISO model (Fig. 5). The TAN model predicts that after about a day the L = 4 flux tube refills with a rate of about ~ 15 cm^{-3}/day, although the refilling rate progressively decreases.

Summarizing the study on the refilling time, we emphasize that the ion temperature anisotropy plays a crucial role in determining the refilling time. If the anisotropy is self–consistently allowed to evolve with the flow, the supersonic stage last a few hours (< 4 hours). At the end of the supersonic stage the flux tube remains depleted, and the forces associated with the density gradients in the depleted flux tube are balanced by the downward anisotropy force for $T_\parallel > T_\perp$. When Coulomb collisions begin to isotropize the plasma, first beginning near the ionospheric boundaries, the second stage of refilling with subsonic flows starts. The refilling with subsonic flows can last over several days as indicated by observations.

This study comparing the results from the TAN and TISO models will soon appear in Geophysical Research Letters [Singh, 1991].

Besides, the above major effort in developing the two-stream TAN model and its applications to refilling processes, we also dealt with some other aspects of refilling. In a recent commentary we contributed to the ongoing debate on the coupling of ion streams at the equator and pointed out the factors distinguishing electrostatic shock formation by ion-ion instability from the hydrodynamic shock arising out of pressure differences [Singh, 1990a]. We have studied the characteristics of the hydrodynamic shocks in interhemispheric flows during the plasmaspheric refilling problem [Singh et al, 1991].

Kinetic Model and Results

Under the reduced budget awarded for the current NSF grant, resources associated with Horwitz went almost entirely toward supporting a research assistantship for Ms. Joyce Lin, a physics graduate student at UAH. Ms. Lin's efforts, as part of what will ultimately be her doctoral dissertation, have been directed toward the incremental development of a kinetic model for the early stage of plasmasphere refilling. Here we shall describe the approach used and results obtained so far.

Although most models describing plasmasphere refilling are hydrodynamic in nature (e.g., Banks et al., 1971; Grebowsky, 1972; Rosner, 1971; Khazanov et al., 1984; Rasmussen and Schunk, 1989), processes which may only be described kinetically may be significant,

perhaps dominant, in the physics of the early, 'collisionless' stage of the refilling process. These include the possible scattering, perpendicular heating and trapping effects of wave–particle interactions on inflowing polar wind ions. A first examination of the effects of perpendicular heating on inflowing ions into the flux tube in terms of 'average motions and energization was pursued by Singh and Hwang (1987).

In the past two years, we have developed a model for the early, 'collisionless' stage of refilling based on the hypothesis that the principal processes for trapping and heating of these incoming ions occurs through wave–particle interactions. Along an L = 4 magnetic field line, we presume a distribution of wave fields/power levels that lead to two types of velocity alterations of individual ions, pitch angle scattering and perpendicular energization. Following the discussion by Singh and Torr (1988), it is presumed that the pitch angle scattering results from ion interactions with left–hand circularly polarized electromagnetic waves, while the perpendicular heating results form broadband fluctuating perpendicular electric fields that have significant power near the ion cyclotron frequency.

Individual ion trajectories are obtained by integrating the equations of motion for the parallel velocities and perpendicular energies. These motions are influenced by gravity, the magnetic mirror force, and the impulses due to the wave–induced scattering and heating. These velocity and energy impulses are calculated each time step that an ion is advanced via velocity–diffusion coefficients $D_{\alpha\alpha}$ and $D_{\perp\perp}$,for the pitch angle scattering and perpendicular heating rates. The expressions given by Singh and Torr (1988) are used to relate these diffusion coefficients to wave power levels. Information on the distribution of wave powers is sparse, but we have generally used levels consistent with observations and/or thermal noise level fluctuations from densities and characteristic thermal energies for superthermal/ring current particles. From various observational considerations (Kintner and Gurnett, 1977; Gurnett et al., 1984; Young, 1983; Olsen et al., 1987), the power spectral levels for perpendicular heating are in the broad range 10^{-9} to 10^{-14} v^2 m^{-2} Hz^{-1}.

Considering wave power level distributions consistent with these general estimates and often with significant concentration at the magnetic equator, we have integrated individual ion trajectories during bounces along the L = 4 field line. Figure 6 shows an example of a trajectory in which a proton was injected at the topside ionosphere and allowed to move through perpendicular heating effects which were highly concentrated at the equator, but no pitch angle scattering was included. The upper panel, which displays the latitude versus time, shows the ion initially becoming trapped at a mirror latitude of about 20°, and then abruptly at a much smaller latitude of ~ 3°. This sudden confined trapping is associated with dramatic and erratic gains in energy of up to 100 eV. The erratic nature of the energy gain and trapping is directly due to the stochastic nature of the energy impulses, which can, during any given time step, be negative.

To directly simulate the early–stage refilling process, we injected polar wind protons in the form of upgoing halves of bi–Maxwellian distributions at the topside ionosphere altitudes at both ends of the L = 4 flux tube. These base distributions are turned on into an initially 'empty' flux tube at t = 0 and left on at constant flux levels. The trajectories for all the ions are integrated forward as they are injected, and the evolution of bulk parameters, such as density, as well as distribution functions, are obtained all along the field line. Figure 7 displays the total number of ions contained in the flux tube as a function of time for four different combinations of wave–particle interaction power levels. Except for the case where both pitch–angle scattering and perpendicular heating are involved at the indicated power levels (case d), the ion content has attained an asymptotic limit by 7–8 hours. For this case, equatorial ion densities exceed 10 ions/cc by twelve hours.

Examination of the distribution functions illustrates further interesting properties of refilling from the kinetic perspective. Figure 8 shows in color–coded formation 'reduced'

distribution functions, at various times after initiation, versus parallel velocity and geocentric distance. About fifteen minutes, the streams from each of the two conjugate ionospheres exhibit significant dispersion, with the fastest particles having traveled across the equator. By thirty minutes, the dispersion is further extended and the fastest ions (~ 38 km/s) have arrived at the opposite hemisphere. After two hours, two oppositely–directed streams are observed across the range of distance and the dispersive features have washed out, owing to the fact that most ions have had sufficient time to execute one full bounce.

There is also some initial energization and trapping around the equator. By five hours after initiation, the two oppositely–directed streams still retain their distinct identity but some broadening of each stream's main distribution is observed and there is an increased superthermal tail especially for the equatorial regions.

Several presentations on this effect have been made Ms. Lin (Lin et al., 1989a, b,; 1990a, b), with her presentation at the San Francisco American Geophysical Union meeting being selected as an outstanding student paper; only four student papers among forty–two in the Solar–Planetary Relationships Section. A short paper for the Monograph on Magnetosphere–Ionosphere Plasma Modeling has been accepted (Lin et al., 1990c).

Very recently, we have incorporated the effects of binary Coulomb collisions and a neutralizing electron fluid into the semi-kinetic model. The incorporation of the Coulomb collisions was particularly inspired by a talk presented by Lemaire (1990) at the Huntsville Plasmasphere Refilling Workshop, who had done some calculations suggesting that multiple small angle collisions of protons with other protons and with electrons along the flux tube would lead to rather large pitch angle scattering and consequent accumulation of ions and accelerated refilling.

The Coulomb collisions were incorporated using a model for computer particle simulations developed by Takizuka and Abe (1977). This model takes account of Debye shielding and tests both by those authors and ourselves demonstrate that both total momentum and energy are conserved.

The neutralizing electron fluid was simulated both by an isothermal Boltzmann distribution similar to that used by, for example, Wilson et al. (1990), as well as a modified version in which a non-uniform electron temperature distribution is assumed. This latter situation has been discussed, for example, by Hultquist (1970) and recently in a semi-kinetic outflow study Ho et al. (1990). In this case the parallel electric field is given by

$$E_{\parallel} = -\frac{k}{e}\left(1 + \frac{\alpha}{2}\right)\frac{dT_e}{dr} - \frac{kT_e}{n_e}\frac{dn_e}{dr} \qquad (14)$$

where k and e are the Boltzmann constant and the magnitude of the electronic charge; T_e is the (non-uniform) electron temperature, and α is taken to be 1.4. In the absence of temperature gradients, the electric field is consistent with the electrostatic potential associated with a Boltzmann distribution of electrons.

Both of the above effects have only recently been put into the model and we are currently undertaking a thorough study of their effects in the refilling process. However, the initial results are extremely intriguing. Figures 10a, b and c show the time-evolution of H^+ density, and parallel and perpendicular temperature as a function of latitude. In this case, the injected H^+ distribution at each topside ionosphere was the upgoing portion of an upward drifting Maxwellian distribution with parallel velocity of 10 km/s and density of 200 ions/cc. In these initial runs, we have not included wave-particle interaction effects and the electron distribution was taken to be isothermal with a temperature of 3000° K. The density profiles in Figure 9a at various times up to about 28 hours after initiation of refilling show that the effects of Coulomb collisions lead to equatorial densities of about 100 particles/cc after a day. Hence, the collisions lead to a rapid accumulation of plasma.

Furthermore, there is no shock formation in this model. The densities fill in smoothly and, to some extent, can be regarded as filling from the low-altitude end upward.

The H^+ perpendicular and parallel temperatures displayed in Figures 9b and c further illustrate the effects of including the Coulomb collisions in the refilling process. The effective parallel temperature in the initial period of refilling is rather high, about 30,000° K. This high value derives from the fact that initially we have two oppositely-directed streams flowing at ~ +/-20 km/s, so that the temperature moment is large even though the individual streams are cold (injected from the ionosphere with 3000° K temperature). As time progresses, the parallel temperatures cool to about 4000° K. This is due to the frictional slowing down of each beam toward coalescence at zero relative drift. In the perpendicular temperatures, one observes the initial distribution having a strong decline from the ionosphere toward the equator owing to the conservation of the magnetic moments. The increase with time of the temperatures is then due to the frictional heating of the ions as the parallel directed flow motion is converted to random parallel and perpendicular energies through the collisions.

Figure 10 shows a simulated pitch-angle/latitude spectrogram of H^+ fluxes from a semi-kinetic model in which we have included wave-particle interactions with strong equatorial heating and an electron temperature distribution with a peak at the magnetic equator. In this case, we have not included Coulomb collisions. We started with a collisionless equilibrium distribution with an isothermal electron distribution at $T_e = 3000°$ K, turned on the wave-particle interactions and then after one hour introduced a "trapezoidal" electron temperature distribution in which the temperature is flat around the magnetic equator at $kT_e = 1$ eV, then declines to 3000° K over a narrow latitudinal range and then stays at this temperature downward to the ionospheric base. As can be seen from equation (14), this electron temperature distribution leads to narrow regions of downward pointing electric fields on either side of the magnetic equator. This spectrogram plots the H^+ number fluxes (in 1.5° wide bins) versus pitch angle and the magnetic latitude about 1 hour after the introduction of this non-uniform electron temperature distribution. As can be seen, this situation results in trapped ion distributions (peak at 90°) around the magnetic equator and double-stream ion distributions with peaks near 0 and 180° outside the equatorial region. This is similar to certain observations of Olsen et al. (1987) (see, for example, Plate 5). Although we believe the physics involved in producing these parallel electric fields may be better represented by a semi-kinetic model in which the electrons are treated as a fluid with temperature anisotropy and perpendicular and parallel heating (see next section), it is nevertheless interesting that our model does reproduce those main features seen in Olsen et al. (1987).

For the special issue of the Journal of Geophysical Research on plasmasphere refilling that we have organized as an outgrowth of our October workshop, we will be submitting two papers dealing with semi-kinetic models for plasmasphere refilling. One of these will deal with the effects of Coulomb collisions on refilling (Wilson et al., 1991), while the other will examine mainly the effects of wave-particle interactions (Lin et al., 1991). These should be submitted by the end of February.

The studies reported above in Sections 2.1 and 2.2 are based on two different models. During the past 18 months these studies have been pursued almost independently as it was the phase of code developments and their applications to some selected problems. In the next section, we have proposed to carry out comparisons between the two models and use the comparison to verify the results from the hydrodynamic model against the more rigorous kinetic model.

REFERENCES

Horwitz, J.L., L.H. Brace, R.H. Comfort and C.R. Chappell, Dual–spacecraft measurements of plasmasphere–ionosphere coupling, J. Geophys. Res., 91, 11203, 1986.

Horwitz, J.L., R.H. Comfort, P. Richards, M.O. Chandler, C.R. Chappell, P. Anderson, W.B. Hanson and L.H. Brace, Plasmasphere–ionosphere coupling II: Ion composition measurements at plasmaspheric and ionospheric altitudes and comparison with modeling results, J. Geophys. Res., 95, 7949, 1990.

Horwitz, J.L., T.E. Moore, B.L. Giles, G.R. Wilson, C.W. Ho, J. Lin and K.R. Swinney, Kinetic features of core plasmas in the magnetosphere: A new generation of observations and simulations, submitted to J. Geomag. Geoelect., 1990.

Horwitz, J.L., Toward a 'quasi–empirical' scenario for plasmasphere refilling based on thermal ion measurements, presented at the Huntsville Workshop of Plasmasphere Refilling, October, 1990.

Lin, J., J.L. Horwitz and K.S. Hwang, An early–stage model for the refilling of the plasmasphere: Effect of turbulent heating and pitch–angle scattering, presented at the Second Workshop on Magnetosphere/Ionosphere Plasma Models, 1989a.

Lin, J., J.L. Horwitz and G.R. Wilson, An early–stage refilling model based on a "kinetic" approach with trapping due to turbulent ion heating, presented at the Fall 1989 San Francisco AGU meeting, EOS, 70, 1297, 1989b.

Lin, J., J.L. Horwitz, G.R. Wilson and C.W. Ho, A model for early–stage plasmasphere refilling based on kinetic approach with wave–particle interactions, presented at Workshop on Plasmasphere Refilling, Huntsville, Alabama, October, 1990a.

Lin, J., J.L. Horwitz, G.R. Wilson and C.W. Ho, An early–stage refilling model based on a kinetic approach with trapping due to ion heating and pitch–angle scattering, submitted for AGU monograph on Magnetospheric Plasma Models, 1990b.

Lin, J., J. L. Horwitz, G. R. Wilson, D. G. Brown, and C. W. Ho, A semi-kinetic model for early-stage plasmasphere refilling, 2: Effects of wave-particle interactions, to be submitted to J. Geophys. Res., 1991.

Singh, N., Role of ion temperature anisotropy in multistage refilling of the outer plasmasphere, Geophys. Res. Lett., in press, 1991.

Singh, N., Role of Electromagnetic noise in the interhemispheric plasma exchange along closed field lines, Advances in Space Res., in press, 1990.

Singh, N. and D.G. Torr, Effects of temperature anisotropy on the interhemispheric plasma transport during plasmaspheric refilling, Geophys. Res. Lett., 17, 925, 1990.

Singh, N., Comment on "Multistream Hydrodynamic Modeling of Interhemispheric Plasma Flow," by C. E. Rasmussen and R. W. Schunk, J. Geophys. Res., 95, 17,272-17,279, 1990.

Singh, N., Plasmasphere refilling issues as seen from models, presented at the Huntsville Workshop on Plasmaspheric Refilling, October 15–16, 1990.

Singh, N., P. Craven, D.G. Torr and P. Richards, Properties of large scale plasma flow

along a closed field line, submitted to J. Geophys. Res., 1991.

Wilson, G. R., J. H. Horwitz, and J. Lin, A semi-kinetic model for early-stage plasmasphere refilling, 1: Effects of Coulomb collisions, to be submitted to J. Geophys. Res., 1991.

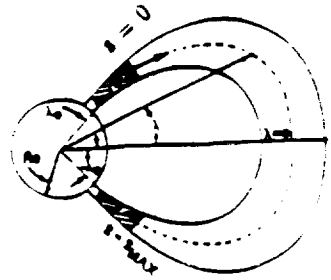

Fig. 1. Geometry of the flux tube. Ionospheric boundaries are at s = 0 (northern ionosphere) and s = s_{max} (southern ionosphere). $\pm\lambda_0$ are the geomagnetic latitudes (λ) of the two boundaries and r_0 is their geocentric altitude.

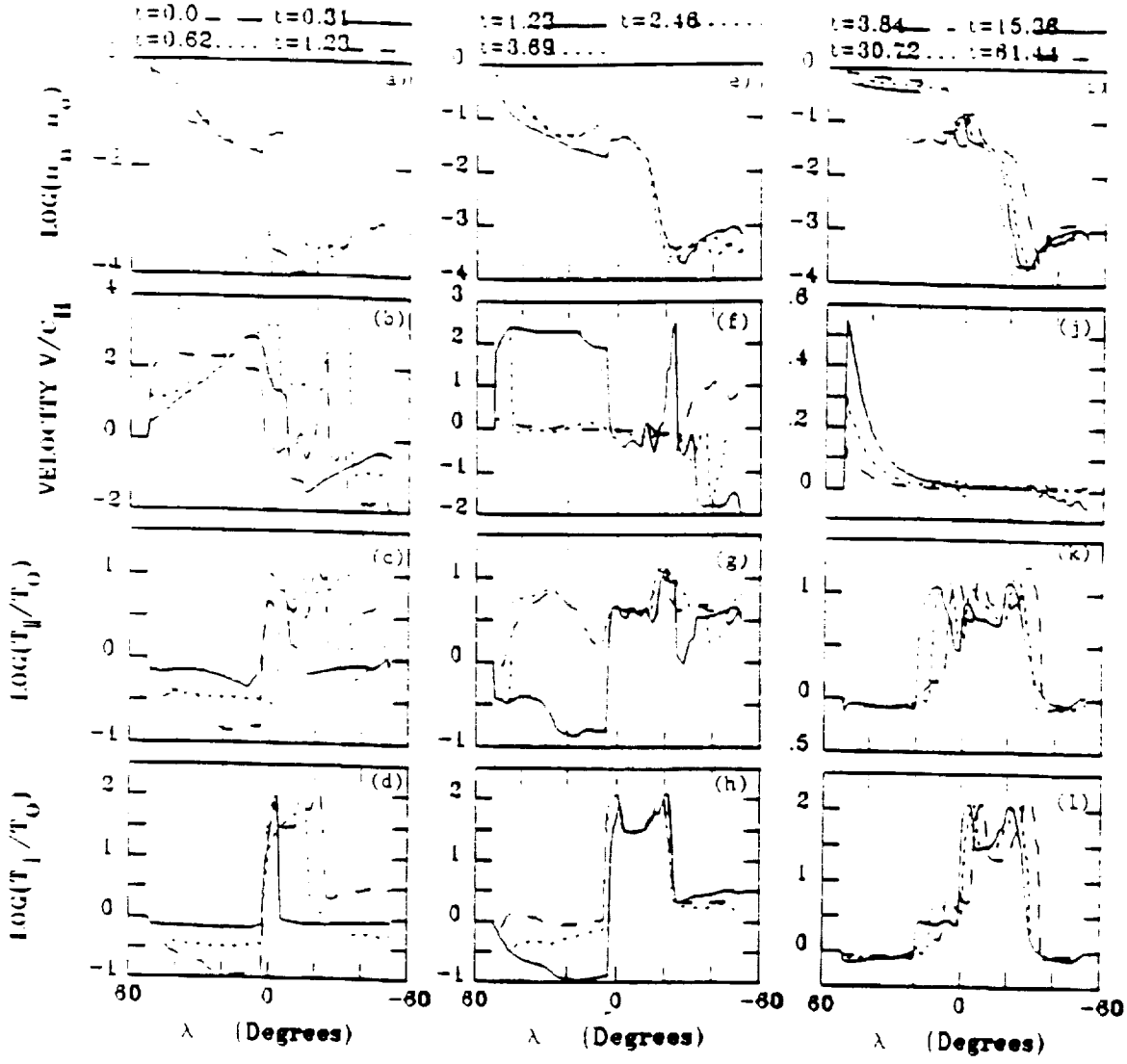

Fig. 2 The early and late time evolutions of the plasma flow developing from the northern hemisphere ($\lambda > 0$). Panels (a) to (d) show the early time profiles of $n_n(\lambda)$, $V_n(\lambda)$, $T_{\perp n}(\lambda)$, and $T_{\parallel n}(\lambda)$, respectively, at some selected times. Panels (e) to (h) show the same quantities at later times. Panels (i) to (ℓ) show the same quantities during the subsonic stage of the flows.

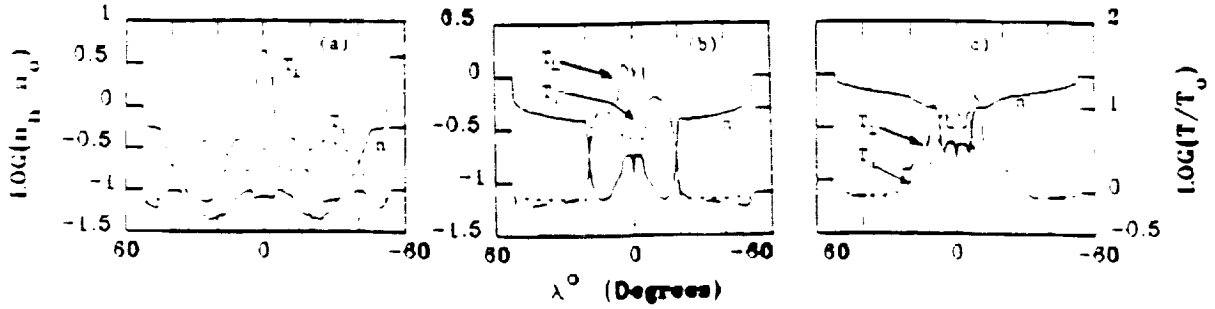

Fig. 3 Evolutions of total density and average temperatures $T_{\perp iv}$ and $T_{\parallel iv}$ are shown. Note the twin-peaked structure in $T_{\perp}$ during the late stage (t = 61.44 hr) of the refilling.

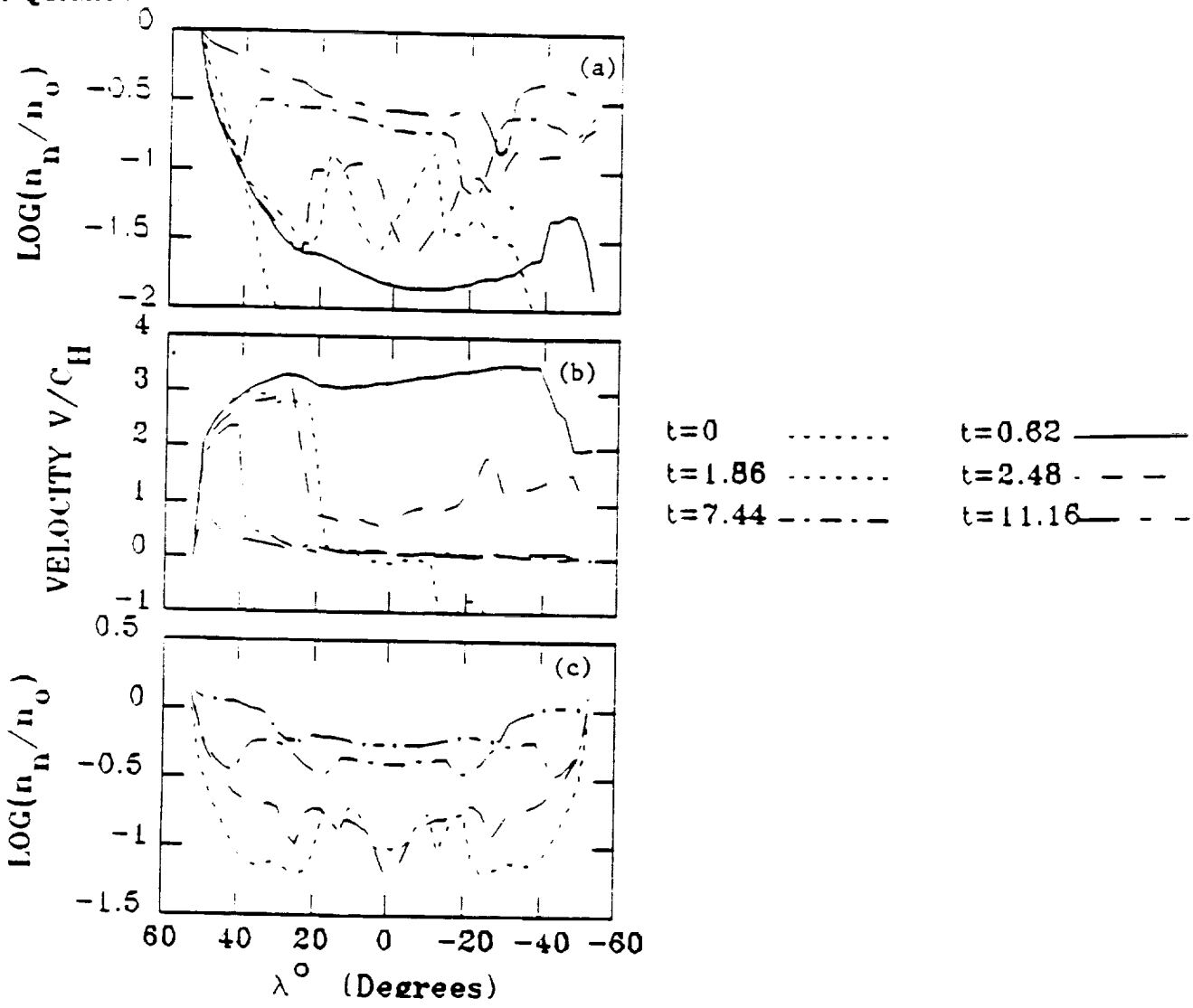

Fig. 4 Refilling as seen from the TISO model. Temporal evolutions of (a) density n_n, (b) low velocity V_n, and (c) total density $n = n_n + n_s$

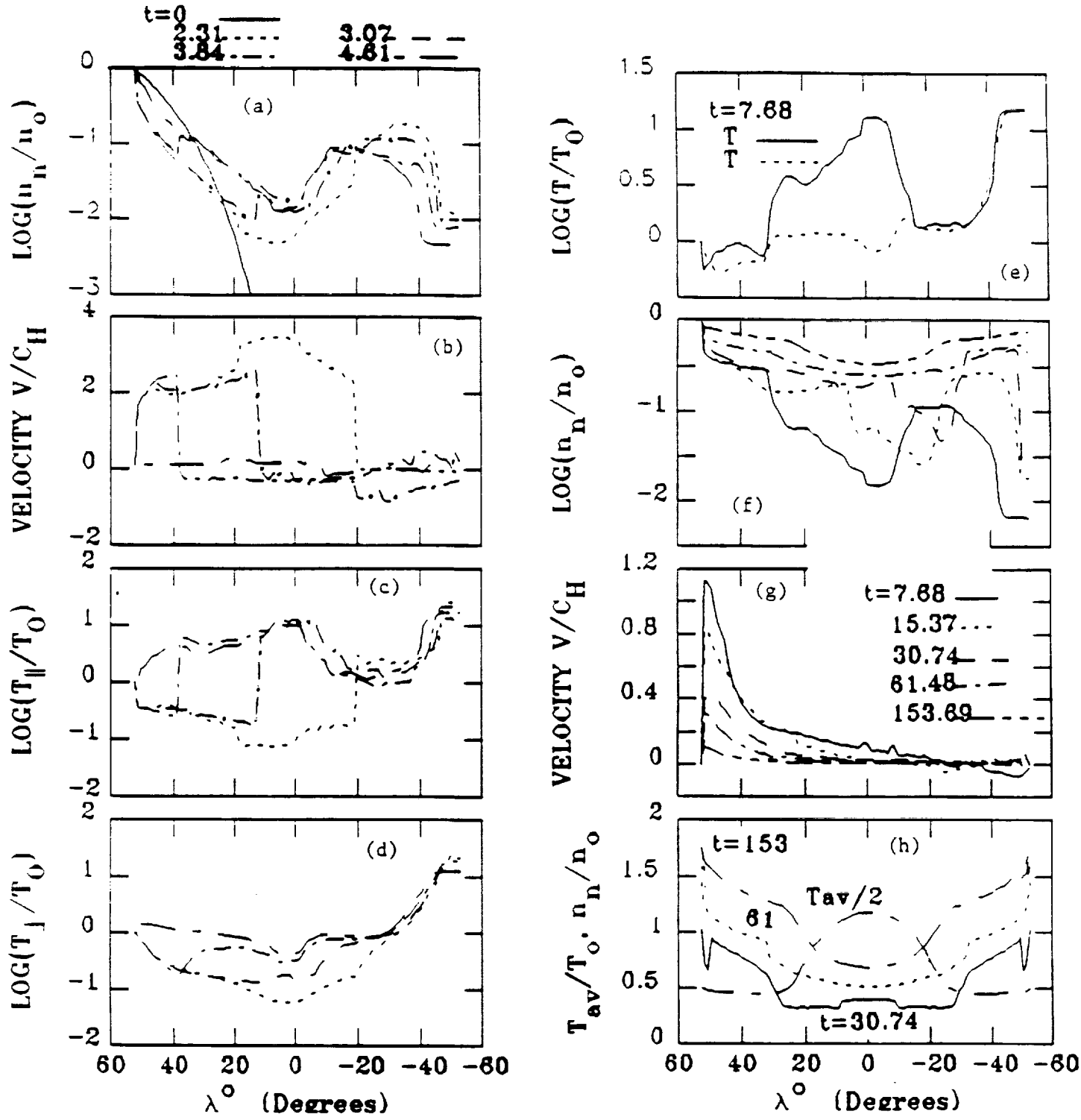

Fig.5. Refilling as seen for the TAN model. Early time temporal evolutions of (a) density n_n, (b) flow velocity V_n, (c) parallel temperature $T_{\|n}$, (d) perpendicular temperature $T_{\perp n}$ are shown up to t = 4.61 hours, when the shock reaches the northern ionospheric boundary, (e) relaxation of the temperature anisotropy near this boundary, (f) evolution of the density ($n_n(\lambda)$) profile at later times, (g) evolution of the velocity profile at later times, and (h) evolution of the total density profile ($n = n_n + n_s$) and the profile of the average temperature T_{av} at t = 153 hr.

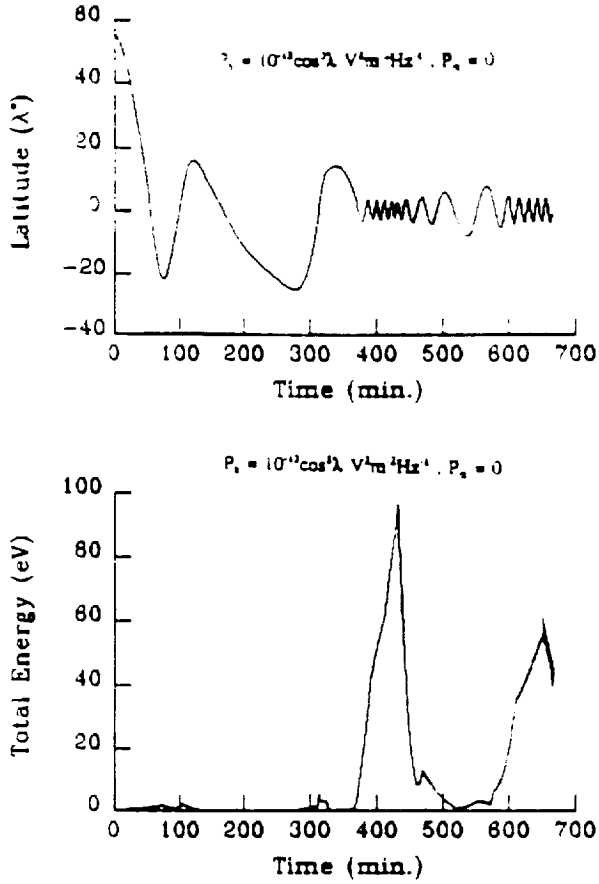

Fig. 6 The time variation of an individual particle's trajectory and total energy with perpendicular heating effect.

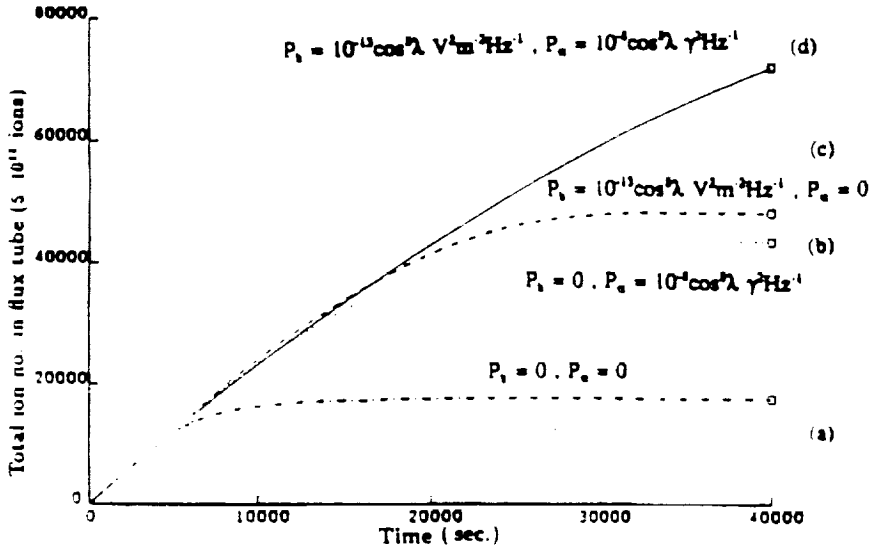

Fig. 7 The time variation of the total number of ions in a flux tube for the four cases of wave-parocle interactions used.

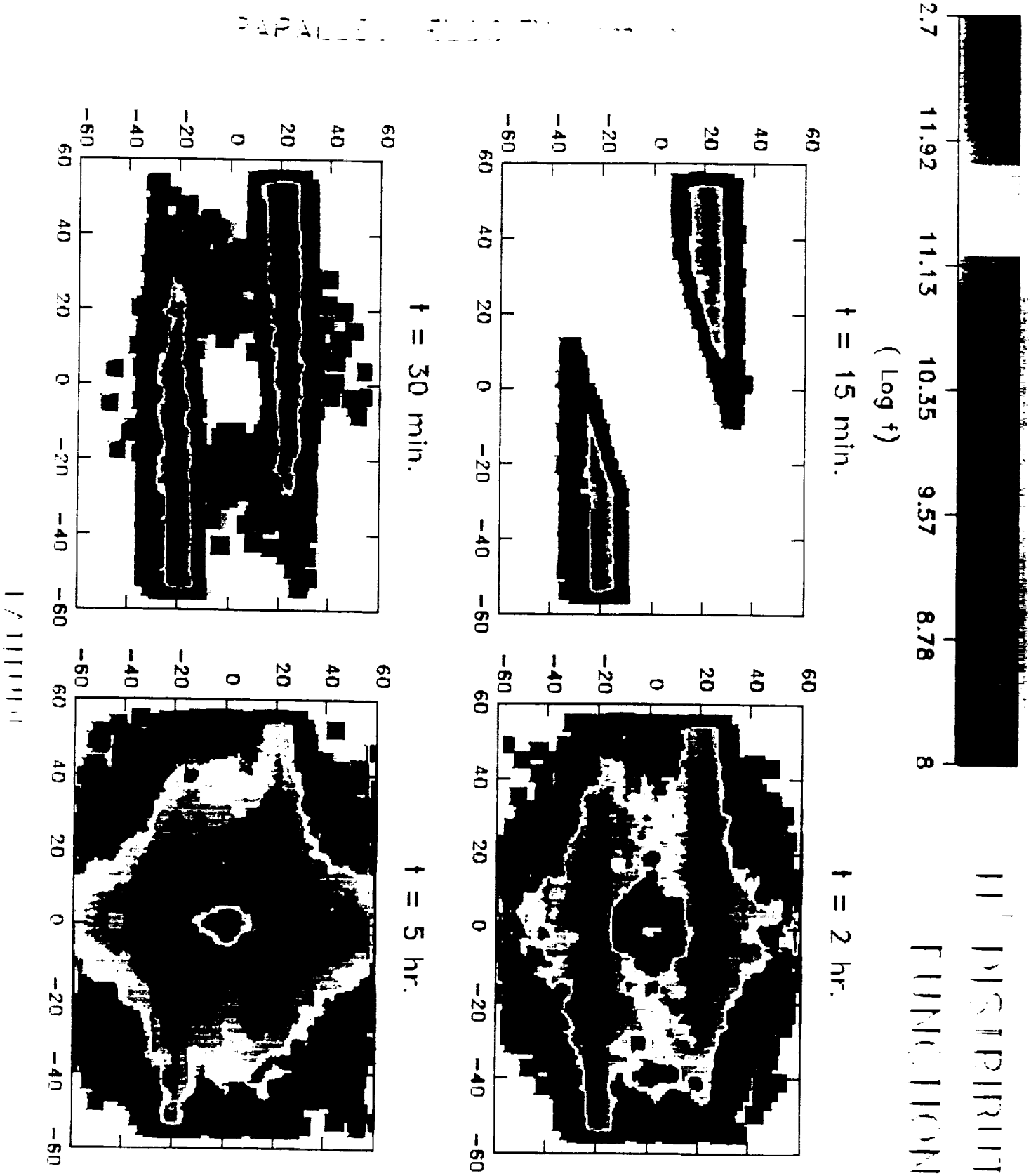

Figure 8. Evolution of the H+ distribution function in kinetic model of early-stage refilling. Each panel depicts the parallel 'reduced' distribution function in color-code spectrogram format versus latitude and parallel velocity (Lin et al., 1991).

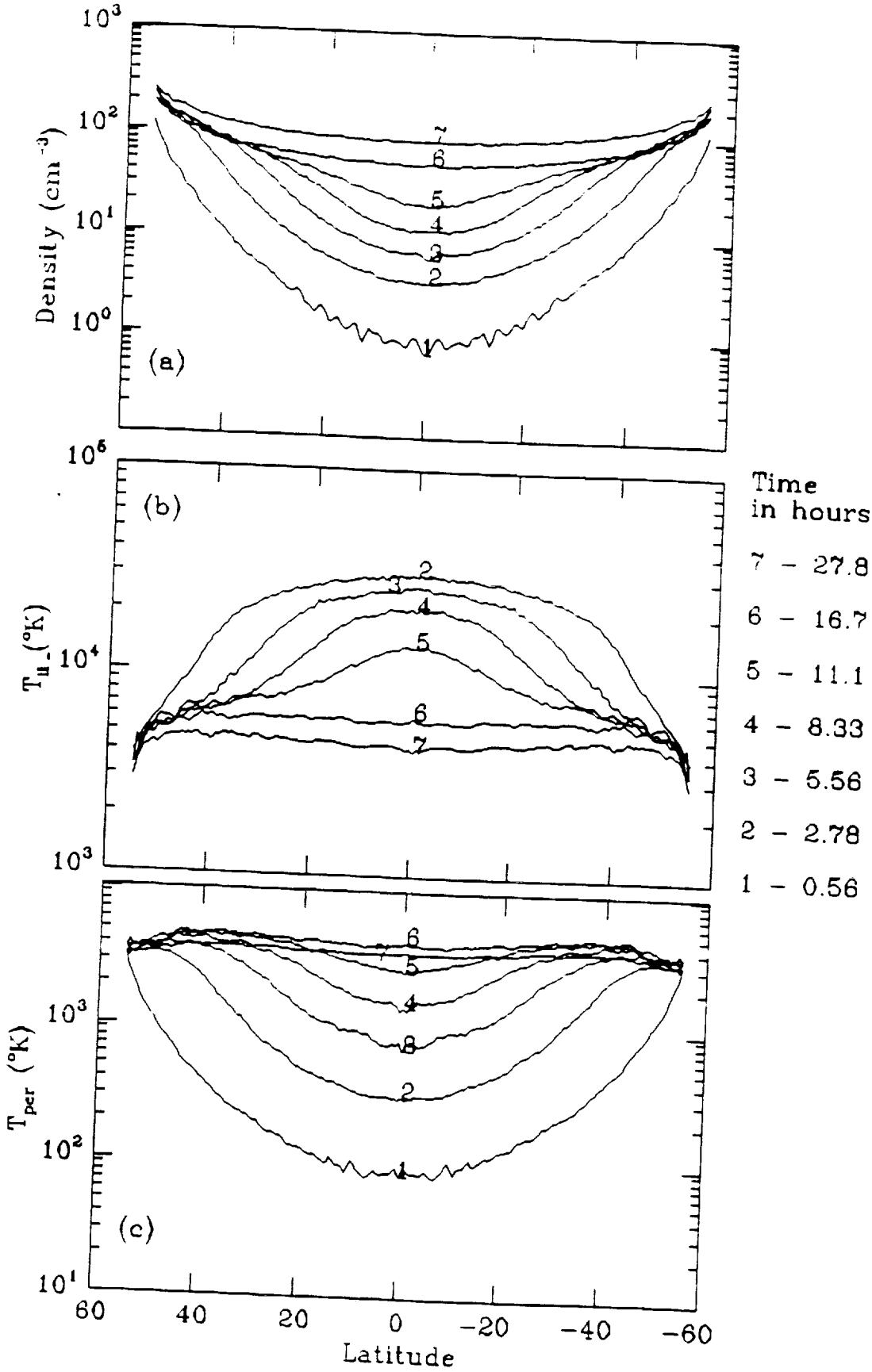

Fig. 9. Plots of the density (a), parallel temperature (b), and perpendicular temperature (c) at the indicated times for the kinetic plasmasphere refilling model which includes the effects of Coulomb collisions but does not include the effects of any wave-particle interactions.

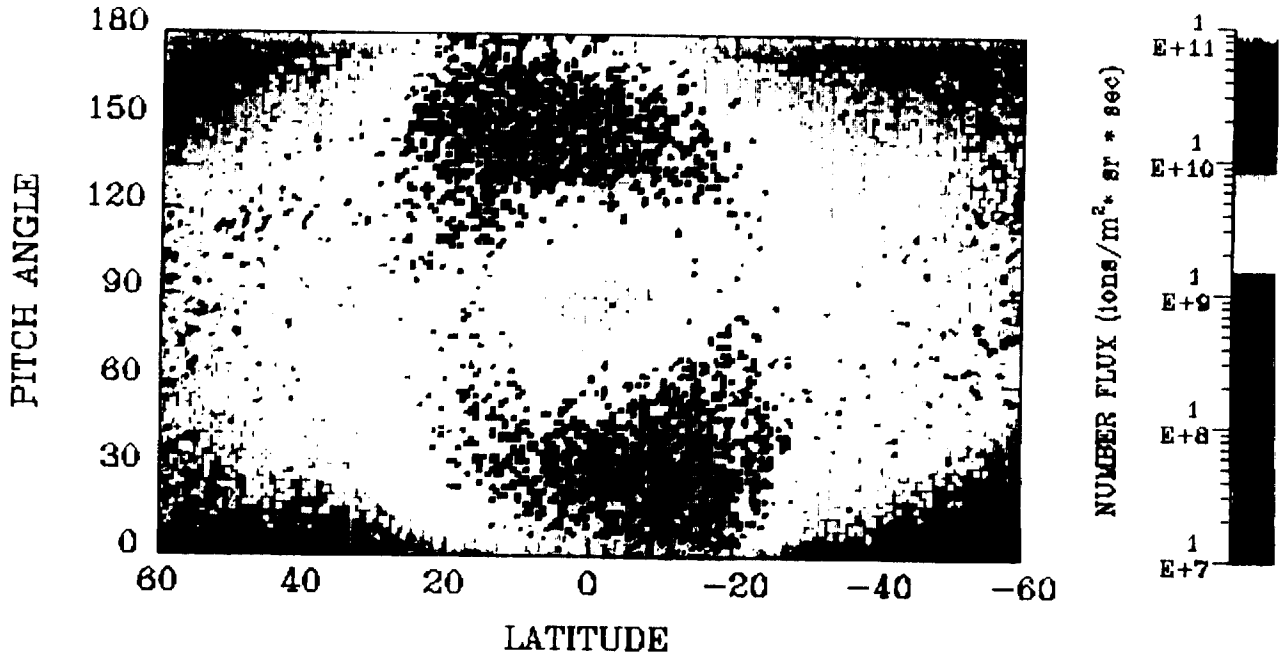

Figure 10. Plot of the (color-coded) H+ differential number flux versus pitch angle and latitude for a late-time snapshot from the semi-kinetic model, illustrating the formation of equatorially-trapped (peak at 90^{o}) ions and field-aligned (peaks at 0^{o} and 180^{o}) streams being reflected from near the equator by electron temperature gradient associated electric fields (Lin et al., 1991)